Journal of Software Engineering

ISSN 1819-4311

Academic Journals Inc.

www.academicjournals.com

Journal of Software Engineering 9 (4): 773-784, 2015
ISSN 1819-4311 / DOI: 10.3923/jse.2015.773.784

Dynamic Modeling and Analysis of a Novel 3-RRR Parallel Shoulder

[1,2]Liang Zhang, [1]Zhenlin Jin and [2]Shuzhen Li
[1]College of Mechanical Engineering, Yanshan University, Qinhuangdao, 066004, China
[2]College of Mechanical and Electronic Engineering, Hebei Normal University of Science and Technology, Qinhuangdao, 066004, China

Corresponding Author: Zhenlin Jin, College of Mechanical Engineering, Yanshan University, Qinhuangdao, 066004, China

ABSTRACT

The dynamic analysis of a novel 3-DOF robot shoulder joint based on orthogonal spherical 3-RRR parallel mechanism was presented. The kinematics constraint equation of this mechanism was established based on the geometric structure and the kinematics model of moving platform was derived. The dynamics model was established based on Lagrange method and the effective inertia, coupling inertia and driving torque of the shoulder joint were analyzed. The variation of the dynamics parameters with the change of the mechanism was discussed and the dynamic coupling relationship between branches was analyzed. The analysis results show that the posture change of the mechanism has a great influence on the dynamics parameters in the process of movement. The results will be useful to improve the control scheme of this mechanism and the selection of servo motor.

Key words: Shoulder, dynamic modeling, virtual work principle

INTRODUCTION

Spherical 3-DOF (degrees of freedom) parallel mechanism is a limited-DOF parallel mechanism which can be widely used for different kinds of practical applications (Zhen *et al*., 2006). It both maintains the inherent advantages of parallel mechanisms and possesses several other advantages in terms of simple structure, low cost in manufacturing and operations. Therefore it has a potentially wide range of applications, such as motion simulator, bionic joint and machine tools. It is attracting the attention of the various researchers and many prototypes based on spherical 3-DOF parallel manipulator have been developed, such as agile eye (Gosselin and Hamel, 1994; Gosselin and St-Pierre, 1997), NC rotary table (Zeng *et al*., 2001), wrist joint (Sun *et al*., 2003), shoulder joint (Jin and Rong, 2007), waist joint (Li and Jin, 2007), bionic eye (Sellaouti *et al*., 2002) etc. The dynamics is an important research content of robot which plays an important role in the, trajectory planning, driver selection and control scheme of the robot (Craig, 2011) and the establishment of the dynamic model for mechanism is the premise and basis for the dynamics analysis of parallel mechanism (Feng *et al*., 2006; Ji *et al*., 2012; Chen *et al*., 2013).

On the basis of the optimal scale parameter values, a novel 3-DOF robot shoulder joint based on orthogonal spherical 3-RRR parallel mechanism is designed but the dynamics of the novel 3-DOF robot shoulder joint is not discussed (Zhang *et al*., 2015), so the dynamic analysis of the robot shoulder joint is presented in this study. Through the analysis and calculation of kinetic energy and potential energy of each component, the dynamics model of the relationship between

driving torque and the motion of the system parameters is established based on Lagrange method. On the basis of the dynamics model, the effective inertia, coupling inertia and driving torque of the parallel mechanism system are analyzed.

MATERIALS AND METHODS

Description of the shoulder: The computer aided design model and schematic of the shoulder joint is shown in Fig. 1 and 2, respectively. The prototype of the shoulder joint in the study is a novel parallel 3RRR orthogonal spherical parallel mechanism. It consists of a fixed platform, a moving platform and three limbs which consist of a framed link and a connecting rod with identical structure. Each limb that consists of three revolute joints in series connects the fixed platform to the moving platform. Thus, the moving platform is attached to the fixed platform by three identical

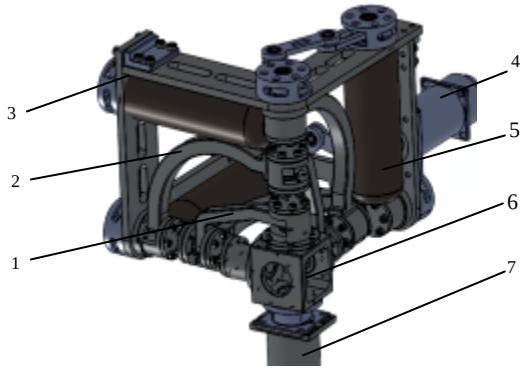

Fig. 1: Prototype of shoulder joint, 1: Connecting rod, 2: Frame link, 3: Frame, 4: Trunk connector, 5: Actuator, 6: Moving platform, 7: Big arm

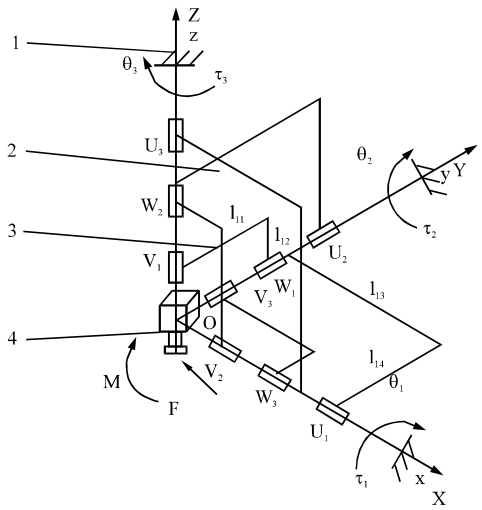

Fig. 2: Schematic diagram of shoulder joint, 1: Fixed base, 2: Frame connecting rod, 3: Connecting rod, 4: Mobile platform

RRR linkages. Nine revolute axes of the mechanism intersect at one point O which is the center of rotation of the spherical body. The axes of three revolute joints connected with the fixed platform are vertical each other and the axes of three revolute joints connected with the moving platform are vertical to each other and the revolute joint axes of framed links and connecting rods are vertical to each other.

Kinematics analysis of the shoulder: Taking the center point O as the origin of the system coordinates, as shown in Fig. 2, a fixed Cartesian frame O{X, Y, Z} connected with the fixed platform and a moving Cartesian frame O{x, y, z} connected with the moving platform are established, with the X, Y, Z axes in coincidence with U_1, U_2, U_3 axes and the x, y, z axes in coincidence with V_1, V_2, V_3 axes, respectively. In the initial posture, the fixed Cartesian frame is coincident with the moving Cartesian frame.

The moving platform only can rotate round the fixed platform, referring to Zhen *et al.* (2006) the transformation matrix between the motion coordinate and the fixed coordinate is given as follows:

$$R = R_{ZYX}(\alpha, \beta, \gamma) = R(Z,\alpha)R(Y, \beta)R(X, \gamma) = \begin{bmatrix} \cos\alpha\cos\beta & \cos\alpha\sin\beta\sin\gamma - \sin\alpha\cos\gamma & \cos\alpha\sin\beta\cos\gamma + \sin\alpha\sin\gamma \\ \sin\alpha\cos\beta & \sin\alpha\sin\beta\sin\gamma + \cos\alpha\cos\gamma & \sin\alpha\sin\beta\cos\gamma - \cos\alpha\sin\gamma \\ -\sin\beta & \cos\beta\sin\gamma & \cos\beta\cos\gamma \end{bmatrix} \tag{1}$$

where, α, β and γ are the posture angles of the mobile platform.
When the moving platform pose changes, the direction cosine U_1, w_i and v_i of revolute joint of the i-th branch (i = 1, 2, 3) can be derived by:

$$\begin{cases} U_i = U_{i0} \\ V_i = RV_{i0} \\ W_i = |U_i \times V_i|^{-1}(U_i \times V_i) \end{cases} \tag{2}$$

where, U_{i0}, W_i and V_{i0} are the direction cosines of revolute joint of the i-th branch (i = 1, 2, 3) when the mechanism is on the initial state.

Referring to Zhen *et al.* (2006) study the constraint equation for the mechanism can be written as follows:

$$W_i \times V_t = 0 \tag{3}$$

Differentiating the constraint Eq. 3 with respect to time, yields:

$$\psi = J\dot{\theta} \tag{4}$$

where, $\dot{\theta} = (\dot{\theta}_1 \ \dot{\theta}_2 \ \dot{\theta}_3)$ is the vector of actuated joint rates and $\psi = (\dot{\alpha}\ \dot{\beta}\ \dot{\gamma})$ is the vector of the output angular velocities of the mechanism. J is the Jacobian matrix of the shoulder mechanism.

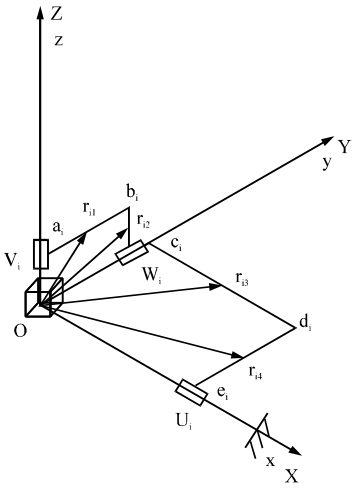

Fig. 3: Sketch of the i-th limb

Dynamic analysis: The schematic diagram of the i-th limb is shown in Fig. 3. The length of a_ib_i and d_ie_i is, l_1, respectively, the length of b_ic_i is l_2, the length of c_id_i is l_3, their linear density is ρ. Then the mass of a_ic_i is $m_{ac} = \rho(l_1+l_2)$, the mass of c_ie_i is $m_{ce} = \rho(l_1+l_3)$.

Kinetic energy analysis: The r_{i1}, r_{i2}, r_{i4} and d_ie_i are arbitrary dots in a_ib_i, d_ie_i, d_ie_i and b_ic_i, respectively, as shown in Fig. 2 and their position vectors can be described as follows:

$$\begin{cases} r_{i1} = l_2 V_i + x_1 W_i, & 0 \le x_1 \le l_1 \\ r_{i2} = l_1 W_i + x_2 V_i, & 0 \le x_2 \le l_2 \\ r_{i3} = l_1 W_i + x_3 U_i, & 0 \le x_3 \le l_3 \\ r_{i4} = l_3 U_i + x_4 W_i, & 0 \le x_4 \le l_1 \end{cases} \tag{5}$$

The kinetic energies of a_ib_i, b_ic_i, c_id_i and d_ie_i are:

$$\begin{cases} T_{iab} = \dfrac{1}{2}\rho\int_0^{l_1} \dot{r}_{i1}^T \dot{r}_{i1} dx_1 \\ T_{ibc} = \dfrac{1}{2}\rho\int_0^{l_2} \dot{r}_{i2}^T \dot{r}_{i2} dx_2 \\ T_{icd} = \dfrac{1}{2}\rho l_3 l_1^2 \left(\dot{W}_i^T \dot{W}_i\right) \\ T_{ide} = \dfrac{1}{6}\rho l_1^3 \left(\dot{W}_i^T \dot{W}_i\right) \end{cases} \tag{6}$$

The kinetic energy of the i-th limb is:

$$\begin{aligned} T_i &= T_{iab} + T_{ibc} + T_{icd} + T_{ide} \\ &= k_1 \dot{V}_i^T \dot{V}_i + k_2 \dot{W}_i^T \dot{W}_i + k_3 \dot{V}_i^T \dot{W}_i \end{aligned} \tag{7}$$

Where:

$$\begin{cases} k_1 = \frac{1}{2}\rho\left(l_1 l_2^2 + \frac{1}{3}l_2^3\right) \\ k_2 = \frac{1}{2}\rho\left(\frac{2}{3}l_1^3 + l_1^2 l_2 + l_1^2 l_3\right) \\ k_3 = \frac{1}{2}\rho\left(l_1^2 l_2 + l_1 l_2^2\right) \end{cases}$$

The total kinetic energy of the three limbs is:

$$T_L = \sum_{i=1}^{3} T_i = \sum_{i=1}^{3}\left(k_1 \dot{V}_i^T \dot{V}_i + k_2 \dot{W}_i^T \dot{W}_i + k_3 \dot{V}_i^T \dot{W}_i\right) \tag{8}$$

The moving platform only can rotate round the fixed platform, so its kinetic energy is:

$$T_D = \frac{1}{2}\dot{\Psi}^T I \dot{\Psi} \tag{9}$$

where, I is a inertia tensor of the moving platform. Based on theoretical mechanics, the following equation can be derived:

$$I = \frac{1}{6}\rho_0 l_2^5 \begin{pmatrix} 1 & 0 & 0 \\ 0 & 1 & 0 \\ 0 & 0 & 1 \end{pmatrix} \tag{10}$$

By substituting Eq. 10 into Eq. 9, the following equation is obtained:

$$T_D = k_4 \dot{\psi}^T \dot{\psi} \tag{11}$$

Where:

$$k_4 = \frac{1}{12}\rho_0 l_2^5$$

In view of Eq. 8 and 11, the total kinetic energy of the mechanism is:

$$T = T_L + T_D = \sum_{i=1}^{3}\left(k_1 \dot{V}_i^T \dot{V}_i + k_2 \dot{W}_i^T \dot{W}_i + k_3 \dot{V}_i^T \dot{W}_i\right) + k_4 \dot{\psi}^T \dot{\psi} \tag{12}$$

Potential energy analysis: Let, position vectors of $a_i c_i$ and $c_i e_i$ be p_{i1} and p_{i2}, respectively, in view of Fig. 2, the position vectors are:

$$\begin{cases} p_{i1} = \begin{bmatrix} W_i & V_i & \dfrac{W_i \times V_i}{|W_i \times V_i|} \end{bmatrix} \begin{bmatrix} x_{ac} \\ y_{ac} \\ 0 \end{bmatrix} = x_{ac} W_i + y_{ac} V_i \\ p_{i2} = \begin{bmatrix} W_i & U_i & \dfrac{W_i \times U_i}{|W_i \times U_i|} \end{bmatrix} \begin{bmatrix} x_{ce} \\ y_{ce} \\ 0 \end{bmatrix} = x_{ce} W_i + y_{ce} U_i \end{cases} \tag{13}$$

where, x_{ac} y_{ac} is the mass center coordinate of a_ic_i in the W_iOV_i plane, x_{ce} y_{ce} is the mass center coordinate of c_ie_i in the W_iOU_i plane.

The potential energy of the i-th limb is:

$$E_i = m_{ac} g p_{i1z} + m_{ce} g p_{i2z} \tag{14}$$

Where:

$p_{i1z} = x_{ac} W_{iz} + y_{ac} V_{iz}$

$p_{i2z} = x_{ce} W_{iz} + y_{ce} U_{iz}$

The total potential energy of the three limbs is:

$$\begin{aligned} E_1 &= \sum_{i=1}^{3} E_i = m_{ac} g \left(\sum_{i=1}^{3} p_{i1z} \right) + m_{ce} g \left(\sum_{i=1}^{3} p_{i2z} \right) \\ &= k_5 (-\sin\alpha \sin\beta \sin\gamma + \cos\alpha \sin\gamma + \cos\alpha \cos\beta) + m_{ce} g y_{ce} \\ &\quad + m_{ac} g y_{ac} (\cos\beta \cos\gamma - \sin\beta + \cos\beta \sin\gamma) \end{aligned} \tag{15}$$

Where:

$k_5 = m_{ac} g x_{ac} + m_{ec} g x_{ce}$

Because the center of mass of the moving platform locates at the origin of the fixed coordinate system, the value of potential energy is 0. Then the total potential energy of the mechanism is:

$$E = E_1 \tag{16}$$

Dynamic modeling: Based on Lagrange method, the dynamic model of shoulder joint can be derived that:

$$f = \frac{d}{dt} \left(\frac{\partial L}{\partial \dot{\psi}} \right) - \frac{\partial L}{\partial \psi} \tag{17}$$

where, $L = T\text{-}E$, in which T is kinetic energy, E is potential energy, $\psi = (\alpha\ \beta\ \gamma)^T$ is generalized coordinates, $f = (f_1\ f_2\ f_3)^T$ is generalized force.

By substituting Eq. 5-16 into Eq. 17, the following equation is obtained:

$$f = \frac{d}{dt} \left(\frac{\partial T_L}{\partial \dot{\psi}} \right) - \frac{\partial T_L}{\partial \psi} + \frac{d}{dt} \left(\frac{\partial T_D}{\partial \dot{\psi}} \right) - \frac{\partial T_D}{\partial \psi} - \frac{d}{dt} \left(\frac{\partial E}{\partial \dot{\psi}} \right) + \frac{\partial E}{\partial \psi} \tag{18}$$

The kinetic equation for the generalized coordinate α can be expressed as:

$$f_1 = k_1\sum_{i=1}^{3}\left(\frac{d}{dt}\left(\frac{\partial\left(\dot{V}_i^T\dot{V}_i\right)}{\partial\dot{\alpha}}\right)-\frac{\partial\left(\dot{V}_i^T\dot{V}_i\right)}{\partial\alpha}\right)+k_2\sum_{i=1}^{3}\left(\frac{d}{dt}\left(\frac{\partial\left(\dot{W}_i^T\dot{W}_i\right)}{\partial\dot{\alpha}}\right)-\frac{\partial\left(\dot{W}_i^T\dot{W}_i\right)}{\partial\alpha}\right)$$
$$+k_3\sum_{i=1}^{3}\left(\frac{d}{dt}\left(\frac{\partial\left(\dot{V}_i^T\dot{W}_i\right)}{\partial\dot{\alpha}}\right)-\frac{\partial\left(\dot{V}_i^T\dot{W}_i\right)}{\partial\alpha}\right)+k_4\frac{d}{dt}\left(\frac{\partial\left(\dot{\psi}^T\dot{\psi}\right)}{\partial\dot{\alpha}}\right)+\frac{\partial E}{\partial\alpha} \quad (19)$$

The kinetic equation for the generalized coordinate β can be expressed as:

$$f_2 = k_1\sum_{i=1}^{3}\left(\frac{d}{dt}\left(\frac{\partial\left(\dot{V}_i^T\dot{V}_i\right)}{\partial\dot{\beta}}\right)-\frac{\partial\left(\dot{V}_i^T\dot{V}_i\right)}{\partial\beta}\right)+k_2\sum_{i=1}^{3}\left(\frac{d}{dt}\left(\frac{\partial\left(\dot{W}_i^T\dot{W}_i\right)}{\partial\dot{\beta}}\right)-\frac{\partial\left(\dot{W}_i^T\dot{W}_i\right)}{\partial\beta}\right)$$
$$+k_3\sum_{i=1}^{3}\left(\frac{d}{dt}\left(\frac{\partial\left(\dot{V}_i^T\dot{W}_i\right)}{\partial\dot{\beta}}\right)-\frac{\partial\left(\dot{V}_i^T\dot{W}_i\right)}{\partial\beta}\right)+k_4\frac{d}{dt}\left(\frac{\partial\left(\dot{\psi}^T\dot{\psi}\right)}{\partial\dot{\beta}}\right)+\frac{\partial E}{\partial\beta} \quad (20)$$

The kinetic equation for the generalized coordinate γ can be expressed as:

$$f_3 = k_1\sum_{i=1}^{3}\left(\frac{d}{dt}\left(\frac{\partial\left(\dot{V}_i^T\dot{V}_i\right)}{\partial\dot{\gamma}}\right)-\frac{\partial\left(\dot{V}_i^T\dot{V}_i\right)}{\partial\gamma}\right)+k_2\sum_{i=1}^{3}\left(\frac{d}{dt}\left(\frac{\partial\left(\dot{W}_i^T\dot{W}_i\right)}{\partial\dot{\gamma}}\right)-\frac{\partial\left(\dot{W}_i^T\dot{W}_i\right)}{\partial\gamma}\right)$$
$$+k_3\sum_{i=1}^{3}\left(\frac{d}{dt}\left(\frac{\partial\left(\dot{V}_i^T\dot{W}_i\right)}{\partial\dot{\gamma}}\right)-\frac{\partial\left(\dot{V}_i^T\dot{W}_i\right)}{\partial\gamma}\right)+k_4\frac{d}{dt}\left(\frac{\partial\left(\dot{\psi}^T\dot{\psi}\right)}{\partial\dot{\gamma}}\right)+\frac{\partial E}{\partial\gamma} \quad (21)$$

Equation 18-20 can be rewritten into the general structure dynamic equation as:

$$f = D\ddot{\psi}+H[\ddot{\psi}^2]+C[\dot{\psi}\,\dot{\psi}]+M \quad (22)$$

where, $\ddot{\psi}=(\ddot{\alpha}\ \ddot{\beta}\ \ddot{\gamma})^T$, $[\dot{\psi}^2]=[\dot{\alpha}^2\ \ \dot{\beta}^2\ \ \dot{\gamma}^2]^T$, $[\dot{\psi}\,\dot{\psi}]=[\dot{\alpha}\dot{\beta}\ \ \dot{\alpha}\dot{\gamma}\ \ \dot{\beta}\dot{\gamma}]^T$, D is the 3×3 symmetric positive equivalent inertia matrix, H is the 3×3 coefficient matrix of centrifugal force, C is the 3×3 coefficient matrix of coriolis force, M is the 3×1 gravity term.

Let input generalized force vector for parallel mechanism be $\tau = (\tau_1\ \tau_2\ \tau_3)^T$. The following equation is obtained via virtual work principle:

$$f = G\tau \quad (23)$$

where, G is force Jacobian matrix of the mechanism. According to dual relationship between motion and force transmissions in mechanism (Craig, 2011) yields:

$$G = J^{-1} \quad (24)$$

Substituting Eq. 24 and 23 into Eq. 22, the following equation is obtained, which is the inverse dynamics equation of the mechanism:

$$\tau = J(D\ddot{\psi} + H[\dot{\psi}^2] + C[\dot{\psi}\,\dot{\psi}] + M) \tag{25}$$

Equivalent inertia analysis: Equivalent inertia has effect on the stability, precision and dynamic response of control system which plays a leading role when the mechanism is accelerated and decelerated. The diagonal elements of the equivalent inertia matrix are also called effective inertia which can be used to estimate the equivalent inertia load of the servo motor. The matrix off-diagonal elements are also called coupling inertia, directly affect the stability of the control system. So, the equivalent inertia determines the dynamic characteristics of mechanism. It is necessary to analyze the equivalent inertia of the mechanism.

The equivalent inertia matrix of parallel shoulder can be derived from Eq. 25, as follows:

$$D = \begin{bmatrix} D_{11} & D_{12} & D_{13} \\ D_{21} & D_{22} & D_{23} \\ D_{31} & D_{32} & D_{33} \end{bmatrix} \tag{26}$$

Where:

$$D_{11} = 4k_1 + k_2(2\cos^2\alpha\sin^2\beta\cos^2\gamma + \sin2\alpha\sin\beta\sin2\gamma + 2\sin^2\alpha\sin^2\gamma + 2\sin^2\alpha\cos^2\beta + 2\sin^2\beta\sin^2\gamma + 2\cos^2\gamma) + 2k_4$$

$$D_{12} = D_{21} = k_2\left(\frac{1}{2}\sin2\alpha\sin2\beta\cos^2\gamma + \frac{1}{2}\sin2\alpha\sin2\beta - \cos^2\alpha\cos\beta\sin2\gamma\right)$$

$$D_{13} = D_{31} = -4k_1\sin\beta - k_2\left(\frac{1}{2}\sin2\alpha\sin^2\beta\sin2\gamma + 2\cos^2\alpha\sin\beta\cos^2\gamma + 2\sin^2\alpha\sin\beta\sin^2\gamma\right) + \frac{1}{2}\sin2\alpha\sin2\gamma + 2\sin\beta$$

$$D_{22} = k_2(2\sin^2\beta\cos^2\gamma + 2\cos^2\alpha\cos^2\beta + 2\cos^2\beta\sin^2\gamma + 2\cos^2\beta + 2\sin^2\alpha\cos^2\beta\cos^2\gamma) + 2k_4 + 4k_1$$

$$D_{23} = D_{32} = k_2\left(\frac{1}{2}\sin2\beta\sin2\gamma + \frac{1}{2}\cos^2\alpha\sin2\beta\sin2\gamma - \sin2\alpha\cos\beta\cos^2\gamma\right)$$

$$D_{33} = 4k_1 + k_2(2\cos^2\beta\sin^2\gamma + 2\cos^2\alpha\cos^2\gamma + 2\sin^2\alpha\sin^2\beta\sin^2\gamma + 2\sin^2\beta\cos^2\gamma + \sin2\alpha\sin2\gamma\sin\beta + 2\sin^2\gamma) + 2k_4$$

According to the discussion above, the equivalent inertia matrix which closely correlates with the sizes of mechanism and density of component is a time-varying function of mechanism configuration and changes with the body posture. This determines the dynamic characteristics of the mechanism.

RESULTS AND DISCUSSION

The structural parameters and inertial parameters of the shoulder are listed in Table 1.

Let motion laws of moving platform of the shoulder joint be as follows:

$$\begin{cases} \alpha = \dfrac{\pi}{6}\sin(6t) & (\text{rad}) \\ \beta = \dfrac{\pi}{6}\cos(6t) & (\text{rad}) \\ \gamma = \dfrac{\pi}{6}\sin(6t) & (\text{rad}) \end{cases} \tag{27}$$

MATLAB (Matrix laboratory) is an interactive software system for numerical computations and graphics. It's a very powerful tool for doing numerical computations with matrices and vectors. Also, it has a variety of capabilities to display information graphically and can be extended through programs written in its own programming language. MATLAB provides a range of numerical computation methods for analyzing data, developing algorithms and creating models. So, the dynamic characteristics indices of the shoulder in task space can be obtained by a developed MATLAB program.

Solving inverse kinematics models, the curves for angular velocities of driving bars are obtained, as shown in Fig. 4. The angular velocities of driving bars regularly change with the

Table 1: Structural parameters and inertial parameters of the shoulder

Parameters	Value
Length of a_ib_i and $d_ie_{il11} = l_{14}$ (mm)	80
Length of b_ic_{il12} (mm)	50
Length of c_id_i l_{13} (mm)	150
Rod linear density ρ (kg m^{-1})	0.63
Moving platform density ρ (kg m^{-3})	2800
Acceleration of gravity (g m^{-1} sec^{-2})	9.8

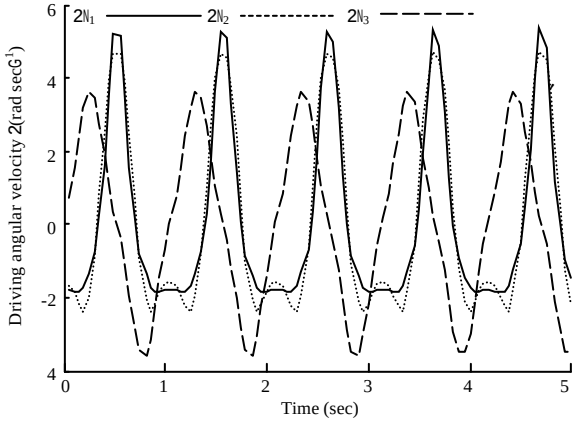

Fig. 4: Curves for driving angular velocities

posture parameters. The angular velocity maximum of the drive rod of branch 1 is 5.371 rad sec^{-1}, the angular velocity maximum of the drive rod of branch 2 is 3.628 rad sec^{-1} and the angular velocity maximum of the drive rod of branch 3 is 4.689 rad sec^{-1}.

Solving the inverse dynamics Eq. 25, the curves for driving torques of driving bars are obtained, as shown in Fig. 5. In the process of movement, the driving torques of the drive rods regularly vary with the changing of posture parameters. The driving torque maximum of the drive rod of branch 1 is 0.4723 Nm, the driving torque maximum of the driving rod of branch 2 is 0.2281 Nm and the driving torque maximum of the drive rod of branch 3 is 0.3558 Nm.

Curves for inertia terms of the mechanism are shown in Fig. 6. It can be observed from Fig. 5 that the equivalent inertia parameters are functions of the parameters of the orientation and change with the mechanism posture. The trends of the equivalent inertia parameters and driving torques are consistent. The variation of the diagonal elements D11 and D33 of the inertia terms are same, their maximum and minimum values are same, respectively. The maximum value is

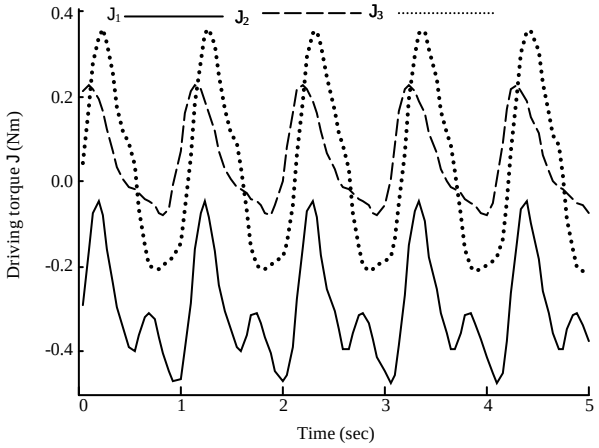

Fig. 5: Curves for driving torques

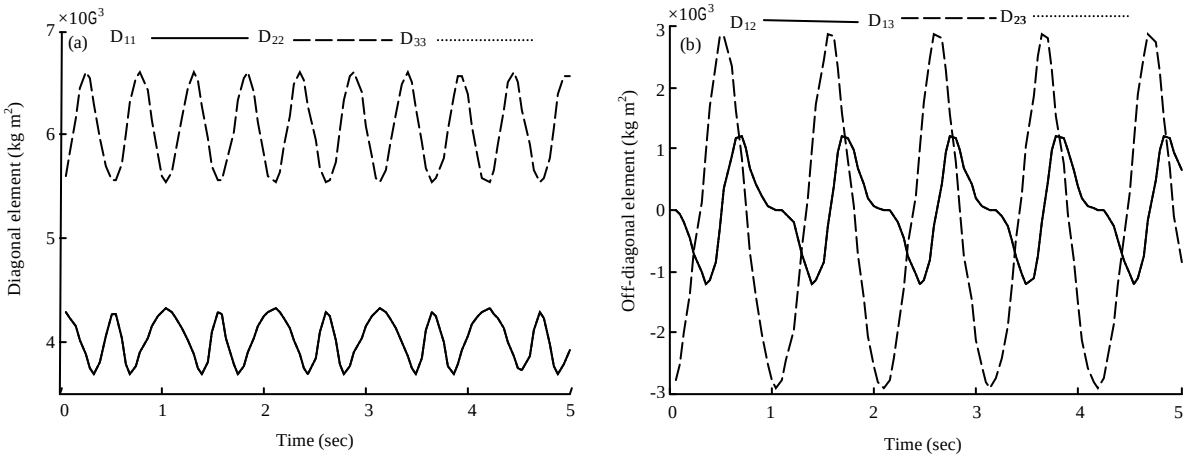

Fig. 6(a-b): Curves for inertia terms, (a) Diagonal element and (b) Off diagonal element

0.0043 kgm^2, the minimum value is 0.0036 kgm^2. The maximum value and minimum value of D22 is 0.0066 kgm^2 and 0.0055 kgm^2, respectively. The effective inertia of branch 2 is larger. The variation of the off-diagonal elements D12 and D23 of the inertia terms are same, their maximum and minimum values are same respectively, their maximum value is 0.0012 kgm^2, the maximum value of D13 is 0.0029 kgm^2. The coupling effect between the branch 1 and branch 3 is larger.

CONCLUSION

Through the analysis and calculation of kinetic energy and potential energy of each component of the novel 3-DOF robot shoulder joint, the dynamics model of the relationship between driving torque and the motion of the system parameters is established based on Lagrange method:

- On the basis of the dynamics model, the effective inertia, coupling inertia and driving torque of the parallel mechanism system are analyzed and the variation of the dynamics parameters of the mechanism is given, the dynamic coupling relationship between branches is analyzed with a developed MATLAB program
- The results show that, the angular velocity and driving torque maximum of the drive rod of branch 1 are the largest, the effective inertia of branch 2 is larger. The coupling effect between the branch 1 and branch 3 is larger and the posture change of the mechanism has a great influence on the dynamics parameters. The results can provide theoretical basis for the mechanism of dynamics optimization design, trajectory planning and control scheme

REFERENCES

Chen, X., W. Feng and Y. Zhao, 2013. Dynamics model of 5-DOF parallel robot mechanism. Trans. Chin. Soc. Agric. Mach., 1: 236-243.

Craig, J.J., 2011. Introduction to Robotics Mechanics and Control. 3rd Edn., China Machine Press, Beijing, China.

Feng, Z., Y. Li, C. Zhang and T.L. Yang, 2006. Present state and perspectives of research on kinematics and dynamics of parallel manipulators. China Mech. Eng., 9: 979-984.

Gosselin, C.M. and J.F. Hamel, 1994. The agile eye: A high-performance three-degree-of-freedom camera-orienting device. Proceedings of the IEEE International Conference on Robotics and Automation, Volume 1, May 8-13, 1994, San Diego, pp: 781-786.

Gosselin, C.M. and E. St-Pierre, 1997. Development and experimentation of a fast 3-DOF camera-orienting device. Int. J. Rob. Res., 16: 619-630.

Ji, Y., H. Liu, D. Yuan and G. Wang, 2012. Analyses for performance indices of a four-DOF parallel manipulator. China Mech. Eng., 3: 258-263.

Jin, Z.L. and Y. Rong, 2007. Design of a waist joint based on three branches unequal spaced distribution spherical parallel manipulator. China Mech. Eng., 18: 2697-2699.

Li, Y.B. and Z.L. Jin, 2007. Analysis and design of input torque of spherical 3-DOF manipulator. Opt. Precis. Eng., 5: 730-735.

Sellaouti, R., A. Konno and F.B. Ouezdou, 2002. Design of a 3 DOFs parallel actuated mechanism for a biped hip joint. Proceedings of the IEEE International Conference on Robotics and Automation, Volume 2, May 11-15, 2002, Washington, DC., USA., pp: 1161-1166.

Sun, L.N., Y. Liu and Y.H. Zhu, 2003. A kinetic analysis of 3-DOF decoupled spherical parallel mechanism used for the wrist joint. China Mech. Eng., 10: 831-834.

Zeng, X., T. Huang, Z. Zeng and Y. Li, 2001. Echanical design of 3-RRR NC rotary table. J. Mach. Des., 4: 13-16.

Zhang, L., Z. Jin and S. Li, 2015. Dimensional synthesis and design of a shoulder joint for fruit and vegetable harvesting manipulator. J. Software Eng., 9: 392-400.

Zhen, H., Z.Y. Sheng and S.T. Zhu, 2006. Advanced Spatial Mechanism. Higher Education Press, Beijing, China, ISBN-13: 9787040192650.